Compact and passive-alignment 4-channel × 25-Gbps optical interconnect modules based on silicon optical benches with 45° micro-reflectors

Article *in* Optics Express · December 2009

DOI: 10.1364/OE.17.024250 · Source: PubMed

CITATIONS
30

READS
508

11 authors, including:

Hsu-Liang Hsiao
Accton Technology
27 PUBLICATIONS **115** CITATIONS

SEE PROFILE

Jin-Wei Shi
National Central University
341 PUBLICATIONS **3,312** CITATIONS

SEE PROFILE

Compact and passive-alignment 4-channel × 2.5-Gbps optical interconnect modules based on silicon optical benches with 45° micro-reflectors

Hsu-Liang Hsiao[1], Hsiao-Chin Lan[1], Chia-Chi Chang[1], Chia-Yu Lee[1], Siou-Ping Chen[1], Chih-Hung Hsu[1], Shuo-Fu Chang[2], Yo-Shen Lin[2], Feng-Ming Kuo[2], Jin-Wei Shi[2], and Mount-Learn Wu[1,*]

[1]Department of Optics and Photonics, National Central University, Jhong-li,32001, Taiwan
[2]Department of Electrical Engineering, National Central University, Jhong-li,32001, Taiwan
**mlwu@dop.ncu.edu.tw*

Abstract: Compact and passive-alignment 4-channel × 2.5-Gbps optical interconnect modules are developed based on the silicon optical benches (SiOBs) of 5 × 5 mm^2. A silicon-based 45° micro-reflector and V-groove arrays are fabricated on the SiOB using anisotropic wet etching. Moreover, high-frequency transmission lines of 4 channel × 2.5 Gbps, and bonding pads with Au/Sn eutectic solder are also deposited on the SiOB. The vertical-cavity surface-emitting laser (VCSEL) array and photo-detector (PD) array are flip-chip assembled on the intended positions. The multi-mode fiber (MMF) ribbons are passively aligned and mounted onto the V-groove arrays. Without the assistance of additional optics, the coupling efficiencies of VCSEL-to-MMF in the transmitting part and MMF-to-PD in the receiving part can be as high as −5.65 and −1.98 dB, respectively, under an optical path of 180 μm. The 1-dB coupling tolerance of greater than ± 20 μm is achieved for both transmitting and receiving parts. Eye patterns of both parts are demonstrated using 15-bit PRBS at 2.5 Gbps.

OCIS codes: (200.4650) Optical interconnects; (130.3990) Micro-optical devices; (230.4040) Mirrors; (130.3120) Integrated optics devices.

References and links

1. B. E. Lemoff, M. E. Ali, G. Panotopoulos, G. M. Flower, B. Madhavan, A. F. J. Levi, and D. W. Dolfi, "MAUI: Enabling fiber-to-processor with parallel multiwavelength optical interconnects," IEEE J. Lightwave Technol. **22**(9), 2043–2054 (2004).
2. S. Hiramatsu, and T. Mikawa, "Optical design of active interposer for high-speed chip level optical interconnects," IEEE J. Sel. Top. Quantum Electron. **24**(2), 927–934 (2006).
3. M. Aljada, K. E. Alameh, Y. T. Lee, and I. S. Chung, "High-speed (2.5 Gbps) reconfigurable inter-chip optical interconnects using opto-VLSI processors," Opt. Express **14**(15), 6823–6836 (2006), http://www.opticsinfobase.org/oe/abstract.cfm?URI=oe-14-15-6823.
4. X. Wang, and R. T. Chen, "Fully embedded board level optical interconnects—From point-to-point interconnection to optical bus architecture," Proc. SPIE **6899**, 6899031–6899039 (2008).
5. D. V. Plant, M. B. Venditti, E. Laprise, J. Faucher, K. Razavi, M. Chateauneuf, A. G. Kirk, and J. S. Ahearn, "256-channel bidirectional optical interconnect using VCSELs and photodiodes on CMOS," IEEE J. Lightwave Technol. **19**(8), 1093–1103 (2001).
6. L. Schares, J. A. Kash, F. E. Doany, C. L. Schow, C. Schuster, D. M. Kuchta, P. K. Pepeljugoski, J. M. Trewhella, C. W. Baks, R. A. John, L. Shan, Y. H. Kwark, R. A. Budd, P. Chiniwalla, F. R. Libsch, J. Rosner, C. K. Tsang, C. S. Patel, J. D. Schaub, R. Dangel, F. Horst, B. J. Offrein, D. Kucharski, D. Guckenberger, S. Hegde, H. Nyikal, C.-K. Lin, A. Tandon, G. R. Trott, M. Nystrom, D. P. Bour, M. R. T. Tan, and D. W. Dolfi, "Terabus: Terabit/second-class card-level optical interconnect technologies," IEEE J. Sel. Top. Quantum Electron. **12**(5), 1032–1044 (2006).
7. R. Heming, L. C. Wittig, P. Dannberg, J. Jahns, E. B. Kley, and M. Gruber, "Efficient planar-integrated free-space optical interconnects fabricated by a combination of binary and analog lithography," IEEE J. Lightwave Technol. **26**(14), 2136–2141 (2008).
8. P. Lukowicz, J. Jahns, R. Barbieri, P. Benabes, T. Bierhoff, A. Gauthier, M. Jarczynski, G. A. Russell, J. Schrage, W. Sullau, J. F. Snowdon, M. Wirz, and G. Troster, "Optoelectronic interconnection technology in the HOLMS system," IEEE J. Sel. Top. Quantum Electron. **9**(2), 624–635 (2003).

#118285 - $15.00 USD Received 7 Oct 2009; revised 14 Dec 2009; accepted 14 Dec 2009; published 18 Dec 2009

9. H. L. Althaus, W. Gramann, and K. Panzer, "Microsystems and wafer processes for volume production of highly reliable fiber optic components for telecom- and datacom-application," IEEE Trans. on Compon. Packag. and Manufact. Technol. pt. B, **21**(2), 147–156 (1998).
10. H. Takahara, "Optoelectronic multichip module packaging technologies and optical input/output interface chip-level packages for the next generation of hardware systems," IEEE J. Sel. Top. Quantum Electron. **9**(2), 443–451 (2003).
11. D. Shimura, R. Sekikawa, K. Kotani, M. Uekawa, Y. Maeno, K. Aoyama, H. Sasaki, T. Takamori, K. Masuko, and S. Nakaya, "Bidirectional optical subassembly with prealigned silicon microlens and laser diode," IEEE Photon. Technol. Lett., vol.18, no.16, pp. 1738–1740, Aug. (2006).
12. Y. Ishii, N. Tanaka, T. Sakamoto, and H. Takahara, "Fully SMT-compatible optical –I/O package with microlens array interface," IEEE J. Lightwave Technol. **21**(1), 275–280 (2003).
13. B. S. Rho, S. Kang, H. S. Cho, H. H. Park, S. W. Ha, and B. H. Rhee, "PCB-compatible optical interconnection using 45°-ended connection rods and via-holed waveguides," IEEE J. Lightwave Technol. **22**(9), 2128–2134 (2004).
14. F. Wang, F. Liu, and A. Adibi, "45 degree polymer micromirror integration for board-level three-dimensional optical interconnects," Opt. Express **17**(13), 10514–10521 (2009), http://www.opticsinfobase.org/oe/abstract.cfm?URI=oe-17-13-10514.
15. S. H. Hwang, J. Y. An, M. H. Kim, W. C. Choi, S. R. Cho, S. H. Lee, H. S. Cho, and H.-H. Park, "VCSEL array module using (111) facet mirrors of a V-grooved silicon optical bench and angled fibers," IEEE Photon. Technol. Lett. **17**(2), 477–479 (2005).
16. I. Zubel, "Silicon anisotropic etching in alkaline solutions III: On the possibility of spatial structures forming in the course of Si(100) anisotropic etching in KOH and KOH+IPA solutions," Sens. Actuators A Phys. **84**(1), 116–125 (2000).
17. H. C. Lan, H. L. Hsiao, C. C. Chang, C. H. Hsu, C. M. Wang, and M. L. Wu, "Monolithic integration of elliptic-symmetry diffractive optical element on silicon-based 45 ° micro-reflector," Opt. Express **17**(23), 20938–20944 (2009), http://www.opticsinfobase.org/oe/abstract.cfm?URI=oe-17-23-20938.

1. Introduction

Optical interconnect technologies at rack-to-rack, board-to-board, and chip-to-chip signal transmission have received great attentions in recent years due to the ever-increasing need for higher bandwidth [1–6]. In order to carry the bandwidth load of board-to-board and processor-to-processor in high-end computer systems, a 500-Gbps parallel wavelength-division multiplexed (PWDM) optical interconnect [1] with 48 channels of 10.42-Gbps data transmitted over a parallel 12-fiber ribbon with 4 wavelength per fiber was demonstrated in the MAUI project funded in part by the DARPA, USA. The optical configuration adopted in such a PWDM module is the planar-integrated free-space optics (PIFSO) [7,8] with integrated coarse wavelength-division multiplexing. A PIFSO system integrates free-space optical elements such as lenses and mirrors on the surfaces of a transparent substrate. Light signals propagating inside the substrate are bounced by the mirrors on zigzag paths along a tilted and folded optical axis. Tolerances of non-coplanar alignments for optical couplings between vertical-cavity surface-emitting lasers (VCSELs), photo-detectors (PDs), and fibers along such tilted and folded optical axes are very tight. The optical subassembly of PIFSO is complicated and should be realized using the active-alignment approach.

As compared to the complicated PIFSO system applied to board-to-board application, a simple optical configuration based on the optical waveguide [6] was developed for chip-to-chip optical interconnects with a data rate of terabit per second. The optical coupling between VCSELs and PDs is based on a single-lens array etched onto the backsides of optoelectronic arrays and on 45° mirrors in the waveguides. In such an optical configuration, VCSELs, PDs, and 45° mirrors in the waveguides form a non-coplanar alignment along two optical axes perpendicular to each other. For achieving a non-coplanar alignment for optical coupling between lasers (LDs), PDs, and fibers (or waveguides) along two optical axes perpendicular to each other, various 45° reflectors including glass micro-prisms [9,10], slanted thin film filters [11], 45° slanted facets on waveguides [6,12,14] or on fiber rods [13] were utilized. Currently, non-coplanar optical deflection is inevitable in most board-to-board or chip-to-chip optical interconnect modules [2–6,12–14].

Since the optical path of LD-to-waveguide (or waveguide-to-PD) is large based on traditional packaging technologies, it is necessary to insert focusing or collimating elements into optical systems to improve the coupling efficiency. Various focusing or collimating elements including UV-curable epoxy resin micro-lenses [12], silicon-based micro-lenses [9],

#118285 - $15.00 USD Received 7 Oct 2009; revised 14 Dec 2009; accepted 14 Dec 2009; published 18 Dec 2009

and silicon diffractive optical elements (DOEs) [11] were applied. It means the active alignment is inevitable to assemble the optical system with a larger optical path for the most optical interconnect modules. Therefore, miniaturizing the optical system would facilitate the optical coupling without adding focusing or collimating elements into such a system. In order to shrink the optical system, a patterned and etched silicon substrate, so-called silicon optical bench (SiOB) [9,11], was implemented as a assembly template for the integration of LDs, PDs, micro-reflectors, micro-lenses, single-mode fibers (or waveguides), and integrated electronics.

Compared to long-distance optical communications, much shorter transmission distances are needed for most board-to-board optical interconnect modules, normally less than 1 meter. Adopting multi-mode waveguides or fibers (with relatively larger core sizes compared to single-mode fibers) as a communication bridge in optical interconnect modules cannot only fit the requirements of ultra-high-speed bit rate transmission, but also have many benefits such as higher coupling efficiency, wider assembly tolerance, and that low costs. Therefore, incorporating the miniature functionality of SiOB technologies as well as using MMFs would be possible that there is no need to use a focusing element between VCSELs/LDs/PDs and MMFs, but that sufficiently high coupling efficiency is achieved.

In this paper, board-to-board 4-channel × 2.5-Gbps optical interconnect modules including transmitting and receiving parts are developed based on the SiOBs, as shown in Fig. 1(a). A silicon-based 45° micro-reflector and V-groove arrays are monolithically integrated on the SiOB using anisotropic wet etching. The VCSEL array and PD array are flip-chip assembled on the intended positions using Au/Sn eutectic bonding. The MMF ribbons are passively aligned and mounted onto the V-groove arrays using the UV curable gel. The 45° micro-reflector is applied to eliminate assembling the glass micro-prism for non-coplanar coupling between the VCSEL array, MMF ribbon, and PD array without additional optics for optical coupling. It would facilitate the optical alignment of non-coplanar light coupling as well as further simplify and miniaturize the volume of microsystem. In addition, the MPO fiber adaptor is adopted here as a pluggable fiber ribbon connector, providing higher flexibility to connection between boards or a computer and peripheral devices. A similar SiOB-based configuration for optical interconnect module has been demonstrated by H. -H. Park *et al.* with a 54.74° micro-reflector of the silicon (111)-plane [15]; however, their fiber facets have to be further treated with a specific angle, which also introduces assembly difficulties. This demonstration still set an example of a compact SiOB-based optical interconnect module.

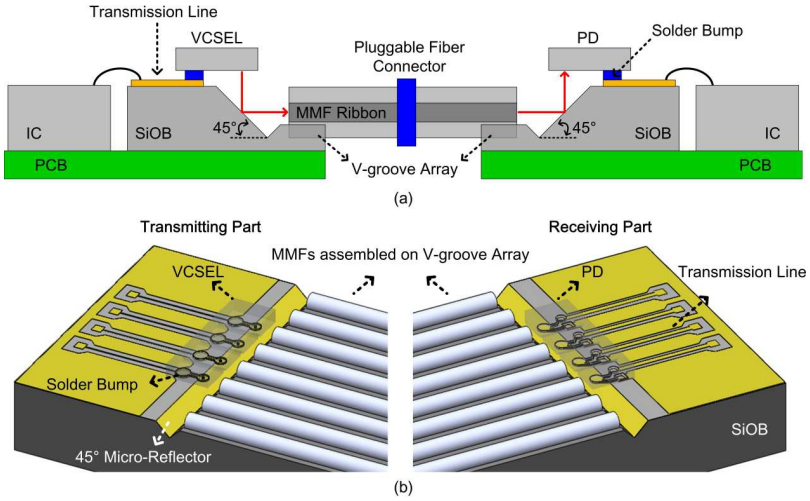

Fig. 1. Schematic diagrams of the proposed optical interconnect module based on the SiOBs. (a) Side-view drawing. (b) top-view drawing.

#118285 - $15.00 USD Received 7 Oct 2009; revised 14 Dec 2009; accepted 14 Dec 2009; published 18 Dec 2009

2. Optical characteristics of SiOB-based optical interconnect modules

The schematic configurations of the proposed SiOB-based optical interconnect modules for transmitting and receiving parts are shown in Fig. 1(b). As can be seen in the figure, the SiOB consists of a 45° micro-reflector and a multi-channel V-groove array. The surface of micro-reflector should reach the optical quality level as the etching depth equal to 104 μm. As shown in the transmitting part, the 4-channel VCSEL array is flip-chip assembled on the top mesa of SiOB using the Au/Sn eutectic solder. The laser beam emitting from the VCSEL array is deflected by the silicon-based 45° micro-reflector and coupled into the MMF ribbon fixed in the V-groove array. The optical path between VCSEL array and fiber ribbon is 180 μm. As shown in the receiving part, the 4-channel PD array is flip-chip assembled on the top mesa of SiOB using the Au/Sn eutectic solder. The laser beam emitting from the MMF ribbon is deflected by the silicon-based 45° micro-reflector and coupled into the PD array. The optical path between PD array and fiber ribbon is also 180 μm. In order to develop a passive alignment configuration for optical interconnect modules, the structure and position of V-groove array should be well controlled to achieve high-precision VCSEL-to-MMF and MMF-to-PD alignments. In addition, the high-frequency transmission lines for electrical signals are also defined on the top mesa of the SiOB.

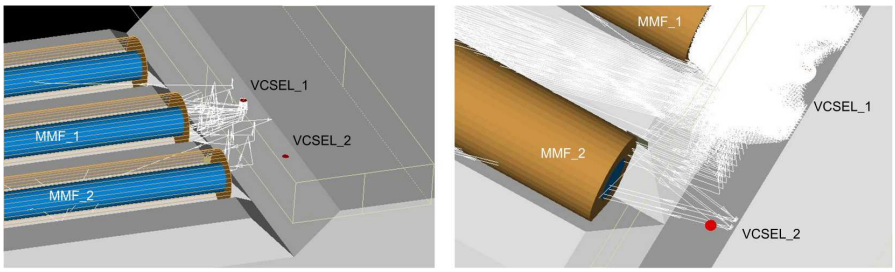

Fig. 2. (a) Ray-tracing simulation results for the transmitter. (b) Simulated estimation for optical cross-talk in the adjacent channel.

In order to evaluate optical characteristics of the proposed optical interconnect modules such as the optical signal level and the inter-channel cross-talk, the ray-tracing simulation is applied in the analysis. As mentioned above, the structure parameters given in the numerical analysis include wavelength of VCSEL array λ_{VCSEL} = 0.85 μm, period of VCSEL array Λ_{VCSEL} = 250 μm, period of PD array Λ_{PD} = 250 μm, top open width of V-groove W_v = 157 μm, depth of the 45° micro-reflector H_{MR} = 104 μm, optical path between VCSEL and MMF (or MMF and PD) L_{OP} = 180 μm, diameter of VCSEL emitting area D_{VCSEL} = 15 μm, numerical aperture of VCSEL NA_{VCSEL} = 0.25, diameter of PD receiving area D_{PD} = 90 μm, diameter of MMF core and cladding equal to 62.5 and 125 μm, respectively, and numerical aperture of MMF NA_{MMF} = 0.25. To simplify the simulation, the intensity apodization emitting from the multi-mode VCSEL array or MMF is assumed to be uniform distribution.

Figure 2(a) shows the ray-tracing simulation results to estimate the optical signal level and the inter-channel cross-talk of a transmitting part. As shown in this figure, there are two VCSELs (VCSEL_1 and VCSEL_2) arranged in the array chip and a set of MMFs fixed in the V-groove array. The VCSEL_1 are assumed to be biased; however, the VCSEL_2 are unbiased. The laser beam emitting from the VCSEL_1 are vertically deflected by the micro-reflector and couples into the MMF1. The VCSEL_1-to-MMF_1 coupling efficiency of −5.85 dB is regarded as the optical signal level in the transmitting part. As considering rays with multiple reflections between surfaces, there are several optical rays scatter within the SiOB and couple into the MMF_2, as shown in Fig. 2(b). The VCSEL_1-to-MMF_2 coupling efficiency of −43.77 dB is regarded as the inter-channel cross-talk of a transmitting part. Based on the same simulation method for the receiving part, the MMF1-to-PD1 and MMF1-

#118285 - $15.00 USD Received 7 Oct 2009; revised 14 Dec 2009; accepted 14 Dec 2009; published 18 Dec 2009

to-PD_2 coupling efficiency of −2.21 and −40.17 dB, respectively, are regarded as the optical signal level and inter-channel cross-talk of a receiving part.

3. Fabrication of SiOB for optical interconnect module

The fabrication procedures of this SiOB are described as below, including the realization of 45° micro-reflectors, V-groove arrays, high-reflection gold coating on the slant, high-frequency transmission lines with bonding pads, and solder bumps for following VCSEL's or PD's flip-chip bonding.

The designed SiOB combined with a 45° micro-reflector and an 8-channel V-groove array would be fabricated on a common (100)-silicon wafer by using anisotropic wet etching. The silicon 45° slants, equivalent to {110} planes on the used (100)-orientated wafer, can be realized via a mixed etchant of aqueous potassium hydroxide (KOH) and isopropyl alcohol (IPA) solutions, which has proved that the etching rate of {110} planes can be effectively suppressed to be relatively lower than {111} planes with an angle of 54.74° to the surface of the silicon [16,17]. The KOH concentration is chosen to ~7M with IPA added to saturation in the etchant. In addition, the etching temperature is set to ~75°C with an etching rate of ~0.5 μm/min. Figure 3 shows the oblique viewing of the fabricated SiOB with monolithic integration of a 45° micro-reflector and an 8-channel V-groove array.

The total etching depth of 104 μm is set according to the requirement of VCSEL-to-MMF (or MMF-to-PD) optical path of 180 μm. As shown in Fig. 4(a), the side-view photo of the 45° micro-reflector indicates the accuracy of etching depth can be controlled within only 5%, and the slanted angle of micro-reflector also can be well controlled within 45 ± 0.5°. In addition, Fig. 4(b) shows the AFM measurement of surface profile for the 45° micro-reflector before/after a gold coating. A 300-nm gold film is deposited on the slant to enhance the reflectance of the incident light. The statistic result indicates the RMS surface roughness of this slant is less than 20 nm, which is better than the 1/10 λ requirement of surface accuracy for optical mirrors.

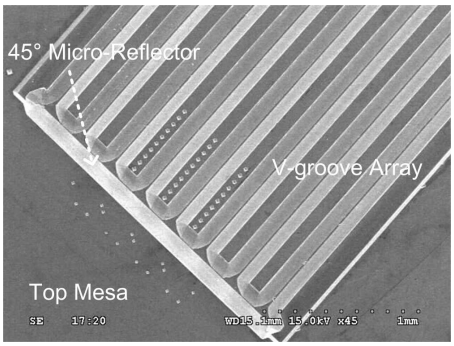

Fig. 3. SEM picture of the fabricated SiOB combined with a 45° micro-reflector and an 8-channel V-groove array. A gold film is deposited on the 45° micro-reflector to enhance the reflectance.

#118285 - $15.00 USD Received 7 Oct 2009; revised 14 Dec 2009; accepted 14 Dec 2009; published 18 Dec 2009

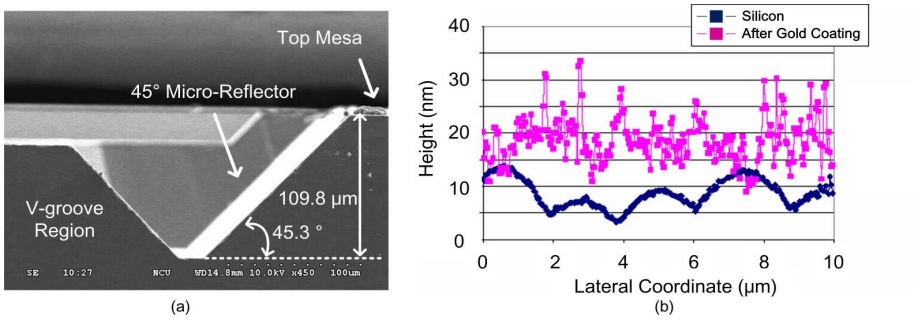

Fig. 4. (a) Side-view photo of the 45° micro-reflector. (b) AFM measurement of the surface profile for the 45° micro-reflector before/after a gold coating.

As shown in Fig. 3, the 8-channel V-groove array with a pitch of 250 μm is fabricated on this SiOB. Although only the 4-channel VCSEL or PD array are used in this study, we detain an expansion possibility of 4 more channels for the higher bit rate requirements based on this SiOB. The cross-sectional picture of this V-groove array is shown in Fig. 5. The slant angle of this V-groove is also very close to 45° because this V-groove array and the 45° micro-reflector are simultaneously fabricated by the same wet-etching process. The top open width of a groove would determine the vertical position of the mounted MMF. Compared to the default width of 157 μm, the fabricated one is approximately 164 μm shown in Fig. 5. Based on the simple geometry, the fiber center *C* in vertical position is calculated as only 3.6-μm misalignment compared to the default position.

After realizing the micro-reflector and the V-groove array, the coplanar waveguide (CPW) transmission lines and Au/Sn solder bumps are fabricated on SiOBs as illustrated in Fig. 6. A SiO_2 dielectric layer of 0.5 μm is sandwiched between the silicon substrate and transmission lines in order to suppress the radiation leakage of electric signals because of the conductivity of silicon. The insertion loss of this CPW transmission line is verified to be 0.88 dB/mm at 2.5 GHz. Its return loss is larger than 30 dB as the signal up to 5 GHz. The inter-channel cross-talk up to 5 GHz is also verified less than 30 dB; therefore, the low interference between transmission lines through high-frequency signals would be obtained. Finally, the Au/Sn bumps are deposited on the pads for the following VCSEL's or PD's flip-chip bonding. As shown in Fig. 6(b), the composition and thickness of Au/Sn solder bump are 80/20 wt% and 2 μm, respectively.

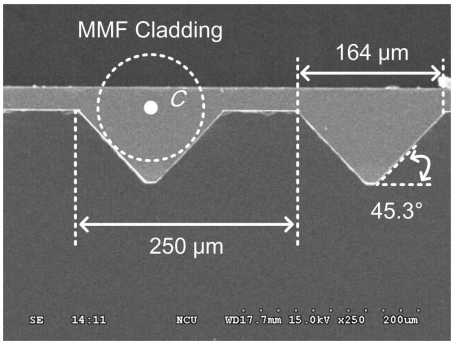

Fig. 5. Side-view photo of the fabricated V-groove array. The fiber center *C* in vertical position is well controlled with only 3.6 μm misalignment.

#118285 - $15.00 USD Received 7 Oct 2009; revised 14 Dec 2009; accepted 14 Dec 2009; published 18 Dec 2009

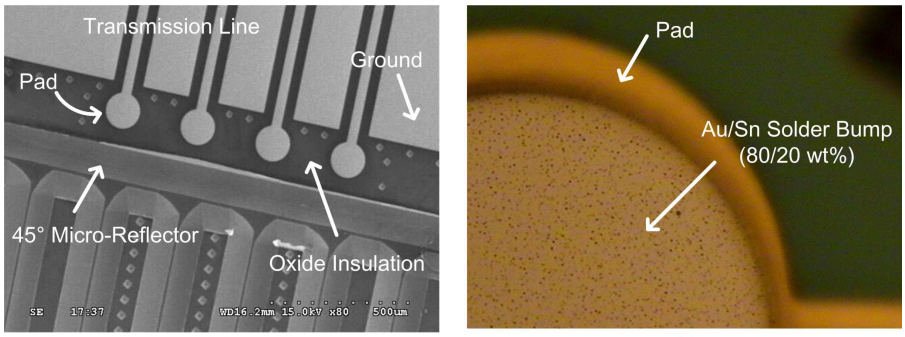

Fig. 6. (a) SEM picture of the fabricated transmission line on the top mesa of the SiOB. (b) Au/Sn solder bump deposited on the pad of the transmission line.

4. Assembly and characterization of optical interconnect modules

The assembly procedures of this optical interconnect module include flip-chip die bonding for the VCSEL array onto the transmitting part and the PD array onto the receiving part as well as the MMF ribbon assembly onto V-groove array. As shown in Fig. 7(a), the 4-channel VCSEL array are flip-chip bonded on the SiOB using Au/Sn eutectic solder bumps. Using the x-ray inspection, the 4-channel VCSEL array flip-chip assembled on the bonding pads as shown in Fig. 7(b) demonstrates the post bonding accuracy is 2 μm. With regard to the pre-treatment of the MMF ribbon, the MMFs are stripped of their jacket and buffer layers, and then the MMFs are cleaved via a standard fiber cleaver without any following AR-coating on the edge of the MMFs. As illustrated in Fig. 8, the MMF ribbon is passively aligned with the VCSEL array and assembled into the V-groove array using a UV-curable gel. A glass lid is adopted to fix the MMF ribbon in the V-groove array during UV curing.

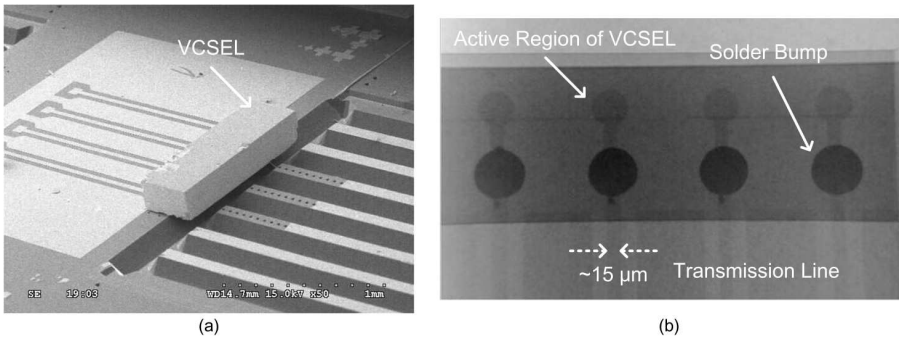

Fig. 7. (a) SEM picture of VCSEL flip-chip bonded on the top mesa of the SiOB. (b) X-ray telescope photo to show the alignment accuracy of VCSEL's flip-chip bonding.

#118285 - $15.00 USD Received 7 Oct 2009; revised 14 Dec 2009; accepted 14 Dec 2009; published 18 Dec 2009

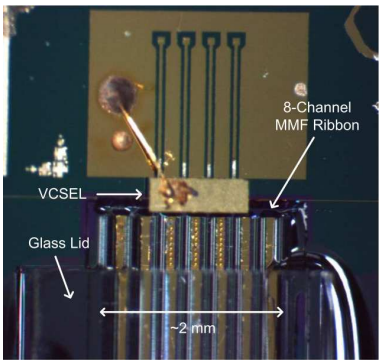

Fig. 8. Photo of 8-channel MMF ribbon mounted on the V-groove array of the SiOB.

In order to study the alignment tolerances of VCSEL-to-MMF and of MMF-to-PD for proposed interconnect modules, the tolerance measurement is carried out by using an active-alignment configuration shown in Fig. 9, the transmitting part for example. This measurement setup consists of a VCSEL array assembled on the SiOB with a 45° micro-reflector and transmission lines only, where the V-groove array has been sawed off from this SiOB. Therefore, the laser beam emitting from a VCSEL impinges upon the 45° micro-reflector and couples into a MMF fixed on a 6-axis moving stage. On the other hand, the active-alignment configure for receiving part consists of a PD array assembled on the SiOB with a 45° micro-reflector only. The V-groove array has also been sawed off from the SiOB. The laser beam emitting from a MMF fixed on a 6-axis stage can impinge upon the 45° micro-reflector and couples into a PD.

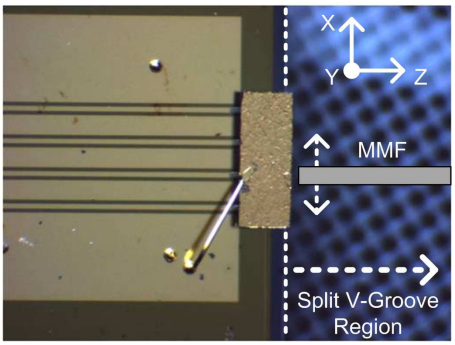

Fig. 9. Schematic of active-alignment tolerance measurement for the proposed interconnect modules.

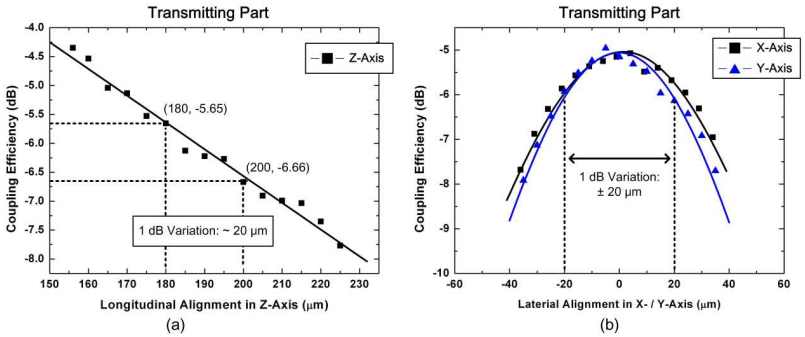

Fig. 10. Alignment tolerance measurement results for the transmitting part.

#118285 - $15.00 USD Received 7 Oct 2009; revised 14 Dec 2009; accepted 14 Dec 2009; published 18 Dec 2009

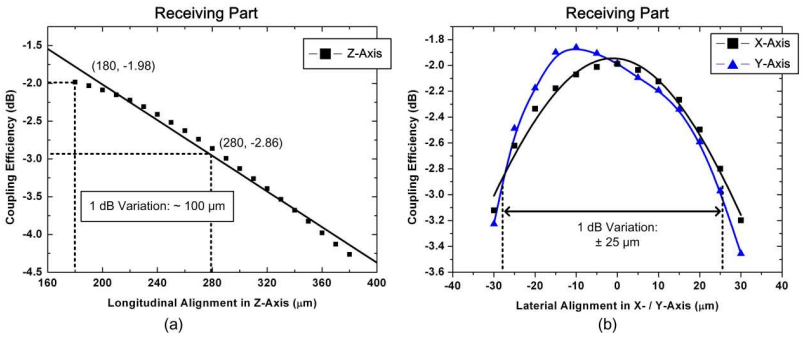

Fig. 11. Alignment tolerance measurement results for the receiving part.

Figures 10(a)-(b) show the measured coupling efficiency of VCSEL-to-MMF versus the longitudinal (Z-axis) and both the lateral (X- and Y-axis) displacements for the transmitting part. As shown in Fig. 10(a), the VCSEL-to-MMF coupling efficiency of −5.65 dB at a working distance of 180 μm is almost the same as the simulated value of −5.85 dB. Its longitudinal alignment tolerance of 1 dB power degradation is approximately 20 μm. Figure 10(b) demonstrates the both lateral alignment tolerances of 1 dB power degradation are about ± 20 μm as the VCSEL-to-MMF working distance is 180 μm. The measurement results verify that the transmitting part possesses the VCSEL-to-MMF coupling efficiency of up to 25% without the assistance of an additional optical element. Its three-dimensional alignment tolerance is around ± 20 μm.

Figures 11(a)-(b) show the measured coupling efficiency of PD versus the longitudinal (Z-axis) and both the lateral (X- and Y-axis) displacements as the laser beam emitting from a MMF couples into a PD. As shown in Fig. 11(a), the PD responsivity of 0.38 A/W at a working distance of 180 μm. Its corresponding MMF-to-PD coupling efficiency is –1.98 dB almost the same as the simulated value of –2.21 dB. Its longitudinal alignment tolerance of 1 dB power degradation is about 100 μm. Figure 11(b) demonstrates the both lateral alignment tolerances of 1 dB power degradation are approximately ± 25 μm as the MMF-to-PD working distance is 180 μm. The measurement results verify that the transmitting part possesses the MMF-to-PD coupling efficiency of up to 65% without the assistance of an additional optical element.

Based on these tolerance measurement results with the active alignment of the MMF, the fabricated 8-channel V-groove with monolithic integration on this SiOB also proves that the provided passive-alignment accuracy is within the tolerance. In the lateral direction (X-axis in Fig. 9), the flip-chip assembled VCSELs/PDs have only 2-μm alignment inaccuracy. In the vertical direction (Y-axis), less than the 3.6-μm misalignment due to the top open width of the silicon V-groove is also within the tolerance. Moreover, the V-groove alignment marks as shown in the central part of Fig. 7(a) would ensure that the MMFs' longitudinal misalignment (Z-axis) is less than 20 μm. Therefore, the three-dimensional alignment tolerance of under the range of ± 20 μm can be achieved by this passive-alignment V-groove sub-mount as well as the accurate flip-chip bonding of VCSEL/PD. In addition, the experimental adjacent-channel cross-talk of this optical interconnect module is also verified down to −35.5 dB and −30.4 dB for transmitting and receiving parts, respectively.

#118285 - $15.00 USD Received 7 Oct 2009; revised 14 Dec 2009; accepted 14 Dec 2009; published 18 Dec 2009

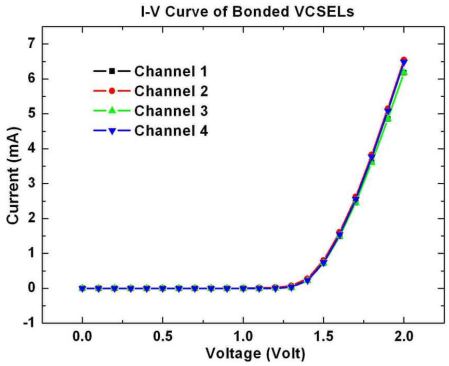

Fig. 12. Measured I-V curve of the 4-channel VCSELs after flip-chip assembled onto the SiOB.

Figure 12 shows the measured I-V curve of the 4-channel VCSEL array after flip-chip assembled onto the SiOB. The 4-channel curves with high consistence indicate that this active element performs well after all the assemble procedures. High-speed optical signal measurements are carried out on both separate parts. The module is tested using planar microwave probes to contact the high speed data input/output interface connected to the VCSEL array or the PD array assembled on the top surface of SiOB. The optical input/output interface is accessed from the MMF fixed onto the V-groove array. A sampling oscilloscope with a 50-GHz bandwidth is adopted to feed the radio-frequency signal. The *Model 1580-B, New Focus* photo detector with a 12-GHz bandwidth is employed for characterizing the transmitting part. Optical eye diagrams are measured at data rate of 2.5 Gbps for the 2^{15}-1 PRBS pattern. The clearly open eyes are demonstrated in Figs. 13(a) and (b) for the transmitting part and receiving part, respectively. Regarding the simultaneous signal transmissions for 4 channels, the clearly open eyes for 4 channels could be anticipated because the adjacent-channel cross-talks between MMFs and high-frequency transmission lines are verified down to –30 dB for both transmitting and receiving part.

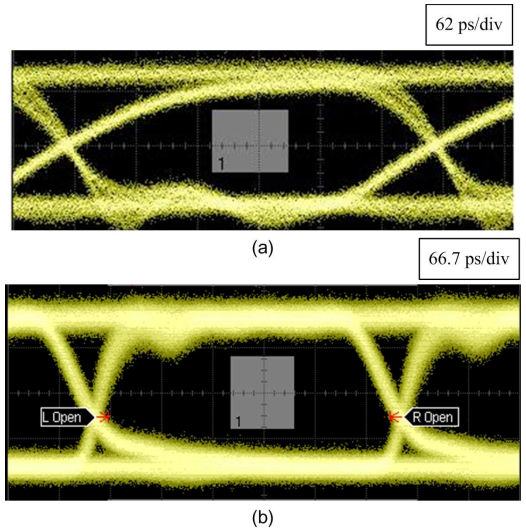

Fig. 13. Eye-diagram results for (a) transmitting part and (b) receiving parts.

#118285 - $15.00 USD Received 7 Oct 2009; revised 14 Dec 2009; accepted 14 Dec 2009; published 18 Dec 2009

5. Conclusion

In this paper, a compact optical interconnect module based on SiOB is developed. By using the SiOB with a 45° micro-reflector, a VCSEL-to-MMF coupling efficiency of −5.65 dB in the transmitting part as well as a MMF-to-PD coupling efficiency of −1.98 dB in the receiving part is achieved without the assistance of additional optics. Moreover, the optical cross-talk between adjacent channels can be suppressed down to under −30 dB. For both parts, the three-dimensional alignment tolerance is at least more than 20 μm, providing relatively larger allowable inaccuracy under the adopted fabrication or assembly variation. The eye diagrams are verified with clearly open eyes at data rate of 2.5 Gbps/channel for both of the transmitting and receiving parts. Furthermore, this optical interconnect module possesses a very compact size in only few millimeter squares, approximately 5 × 5 mm^2 for a single transceiver or receiver. Therefore, it is also suitable for embedding into portable devices in versatile consumer applications.

By using this compact SiOB-based optical interconnect module, the transmission rate over 10 Gbps per channel is also possible as long as the high-frequency transmission lines and the VCSEL/PDs could be replaced to achieve 10-GHz requirements. The short optical paths between VCSEL/PDs and MMFs, as well as the silicon V-groove array also facilitate the coupling issues, the high accurate assemblies, and the passive alignment requirements. Currently, the authors are developing a 4-channel × 10 Gbps optical interconnect module via this SiOB to meet the 10-Gbps/channel expectations of Intel's Light Peak module. The corresponding research results will be published soon.

Acknowledgements

This work was supported by Ministry of Economic Affair of the Republic of China under grant number 96-EC-17-A-07-S1-001.

#118285 - $15.00 USD Received 7 Oct 2009; revised 14 Dec 2009; accepted 14 Dec 2009; published 18 Dec 2009